Hindawi
Journal of Function Spaces
Volume 2023, Article ID 2726735, 11 pages
https://doi.org/10.1155/2023/2726735

Research Article

Reproducing Kernel Method with Global Derivative

Nourhane Attia,[1] **Ali Akgül**,[2,3,4] **and Abdon Atangana**[5,6]

[1]*National High School for Marine Sciences and Coastal (ENSSMAL), Dely Ibrahim University Campus, Bois des Cars, B.P. 19, 16320, Algiers, Algeria*
[2]*Department of Computer Science and Mathematics, Lebanese American University, Beirut, Lebanon*
[3]*Siirt University, Art and Science Faculty, Department of Mathematics, 56100 Siirt, Turkey*
[4]*Near East University, Mathematics Research Center, Department of Mathematics, Near East Boulevard, PC: 99138, Nicosia/Mersin 10, Turkey*
[5]*Institute for Groundwater Studies, Faculty of Natural and Agricultural Sciences, University of the Free State, South Africa*
[6]*Department of Medical Research, China Medical University Hospital, China Medical University, Taichung, Taiwan*

Correspondence should be addressed to Nourhane Attia; n.attia@enssmal.dz

Received 19 May 2022; Accepted 2 September 2022; Published 19 May 2023

Academic Editor: Yusuf Gurefe

Ordinary differential equations describe several phenomena in different fields of engineering and physics. Our aim is to use the reproducing kernel Hilbert space method (RKHSM) to find a solution to some ordinary differential equations (ODEs) that are described by using the global derivative. In this research, we used the RKHSM to construct new numerical solutions for nonlinear ODEs with global derivative. The used method systematically produces analytic and approximate solutions in the series's form. We tested three applications for showing the performance of the RKHSM.

1. Introduction

In the last decades, the rate of change has been increasingly used for understanding the instantaneous changes that arise in widespread fields. Thinking of the derivative as representing a rate of change is very useful when solving physics problems. The derivative plays a fundamental role in forming the ordinary differential equations (ODEs) that are of great importance because of their ability to describe numerous phenomena in physics, such as electrical networks, oscillating and vibrating systems, satellite orbits, and chemical reactions. Finding the ODEs' solutions is the key to understanding nature, but it is hard and sometimes impossible to get the exact solutions of most real-life ODEs, especially the nonlinear ones. And for such a case, one resorts to numerical methods.

The RKHSM is a widely used numerical method for solving nonlinear ODEs (NODEs). This method which was proposed in 1908 [1] is an effective numerical method for complex nonlinear problems without discretization. Many researchers applied it to solve several types of equations [2–14]. The principal advantages of this method are

(1) the feature that is it is easy to be applied, especially because it is meshfree

(2) its capability to deal with diverse complex differential equations

(3) the uniform convergence between the numerical and exact solutions as well as their derivatives

This research aims to provide a new convenient method using the reproducing kernel (RK) theory for obtaining the solution of some nonlinear ODEs that are described by using the global derivative.

In this paper and for the first time, the RKHSM is used for constructing numerical solutions for the nonlinear ODEs with global derivative.

The next section shows some basic definitions and theorems concerning RK theory and global derivative. The

description of the RKHSM and its application to the proposed problem are presented in the third section. The RKHSM's effectiveness and the solutions' accuracy are validated through three applications in the fourth section. Finally, the conclusion is given.

2. Preliminaries

This section covers the theory required to understand the RKHSM we will apply to solve some important nonlinear ODEs with global derivative.

Definition 1. A global derivative of a differentiable function f is [15]

$$D_g f(x) = \lim_{x_1 \longrightarrow x} \frac{f(x_1) - f(x)}{g(x_1) - g(x)}, \tag{1}$$

in which the function g is an increasing nonzero.

Remark 2. If the function g is differentiable then [15]

$$D_g f(x) = \lim_{x_1 \longrightarrow x} \frac{((f(x_1) - f(x))/(x_1 - x))}{((g(x_1) - g(x))/(x_1 - x))} = \frac{f'(x)}{g'(x)}. \tag{2}$$

Remark 3. The global derivative covers the following three cases that we are going to deal with throughout the numerical part:

(1) Case 1: let us choose $g(x) = x$:

$$D_g f(x) = \frac{f'(x)}{g'(x)} = \frac{f'(x)}{(x)'} = \frac{f'(x)}{1} = f'(x). \tag{3}$$

Hence, the classical derivative is a special case of global derivative.

(2) Case 2: let us choose $g(x) = x^\alpha$:

$$D_g f(x) = \frac{f'(x)}{g'(x)} = \frac{f'(x)}{(x^\alpha)'} = \frac{1}{\alpha x^{\alpha-1}} f'(x). \tag{4}$$

Hence, the fractal derivative is a special case of global derivative.

(3) Case 3: let us choose g(x) = sin (x):

$$D_g f(x) = \frac{f'(x)}{g'(x)} = \frac{f'(x)}{(\sin(x))'} = \frac{1}{\cos(x)} f'(x). \tag{5}$$

Definition 4. A function $K : X \times X \longrightarrow \mathbb{C}$ which satisfies

(1) $K(\cdot, x) \in H$ for all $x \in X$

(2) $\langle f, K(\cdot, x)\rangle = f(x)$ for all $f \in H$ and for all $x \in X$

is called a reproducing kernel of H ; H is a Hilbert space over $X \neq \varnothing$.

Definition 5. We set [16].

$$W_2^2[0, T] = \left\{ f(x) | \text{The functions } f \text{ and } f' \text{ are absolutely continuous in } [0, T], f'' \in L^2[0, T], \text{and } f(0) = 0 \right\}. \tag{6}$$

An inner product on $W_2^2[0, T]$ is

$$\langle f, g\rangle_{W_2^2} = \sum_{i=0}^{1} f^{(i)}(0) g^{(i)}(0) + \int_0^T f''(x) g''(x) dx, \tag{7}$$

and its norm is denoted by

$$\|f\|_{W_2^2} = \sqrt{\langle f, f\rangle_{W_2^2}}, \tag{8}$$

for all $f, g \in W_2^2[0, T]$.

Theorem 6. *The function*

$$S_\tau(x) = \begin{cases} x\tau + \frac{1}{2}x^2\tau - \frac{1}{6}x^3 & , x \leq \tau, \\ \tau x + \frac{1}{2}\tau^2 x - \frac{1}{6}\tau^3 & , x > \tau, \end{cases} \tag{9}$$

is the reproducing kernel function of $W_2^2[0, T]$,

For the proof of this theorem, see [17].

Definition 7. We set [16].

$$W_2^1[0, T] = \left\{ f(x) | f \text{ is absolutely continuous in } [0, T] \text{ and } f' \in L^2[0, T] \right\}. \tag{10}$$

An inner product on $W_2^1[0, T]$ is

$$\langle f, g\rangle_{W_2^1} = f(0)g(0) + \int_0^T f'(x)g'(x)dx, \tag{11}$$

and its norm is denoted by

$$\|f\|_{W_2^1} = \sqrt{\langle f, f\rangle_{W_2^1}}, \tag{12}$$

for all $f, g \in W_2^1[0, T]$.

Theorem 8. *The function*

$$R_\tau(x) = \begin{cases} 1 + x & , x \le \tau, \\ 1 + \tau & , x > \tau, \end{cases} \tag{13}$$

is the reproducing kernel function of $W_2^1[0, T]$.

For the proof of this theorem, see [17].

3. Solution Methodology

We now consider the 1st-order nonlinear ODE,

$$\begin{cases} D_g f(x) = F(x, f(x)), \quad x \in [0, T], T \in \mathbb{R}^*, \\ f(0) = \lambda, \end{cases} \tag{14}$$

where D_g is the global derivative, f is the unknown, F is a function of x and $f(x)$, and λ is a constant.

To apply the RKHSM, let us begin with making a change of variable to homogenize the initial condition $f(0) = \lambda$:

$$u(x) = f(x) - \lambda. \tag{15}$$

Replacing $f(x)$ by $u(x) + \lambda$ in (14) gives

$$\begin{cases} D_g u(x) = \bar{F}(x, u(x)), \quad x \in [0, T], T \in \mathbb{R}^*, \\ u(0) = 0, \end{cases} \tag{16}$$

where $\bar{F}$ is a nonlinear function of x and $u(x)$.

The second step is to define a linear operator $\mathrm{A} : W_2^2[0, T] \longrightarrow W_2^1[0, T]$ such that

$$\mathrm{Au}(x) = D_g u(x). \tag{17}$$

We use this linear operator to get

$$\begin{cases} \mathrm{Au}(x) = \bar{F}(x, u(x)), \quad x \in [0, T], T \in \mathbb{R}^*, \\ u(0) = 0. \end{cases} \tag{18}$$

The next step is to build an orthogonal function system of $W_2^2[0, T]$. Let

$$\psi_{\mathrm{i}}(\mathrm{x}) = \mathrm{A}^* \kappa_{\mathrm{i}}(\mathrm{x}), \tag{19}$$

where

(i) $\kappa_{\mathrm{i}}(\mathrm{x}) = R_{\mathrm{x_i}}(\mathrm{x})$; $R_{\mathrm{x_i}}(\mathrm{x})$ represents the RK function of $W_2^1[0, T]$

(ii) The set $\{\mathrm{x_i}\}_{\mathrm{i=1}}^{\infty}$ is dense in $[0, T]$

(iii) A^* is the adjoint of A

Now, to find $\{\bar{\psi}_{\mathrm{i}}\}_{\mathrm{i=1}}^{\infty}$, we need to use Gram-Schmidt's process:

$$\bar{\psi}_{\mathrm{i}}(\mathrm{x}) = \sum_{k=1}^{\mathrm{i}} \varpi_{\mathrm{i}k}\psi_k(x), \quad \varpi_{\mathrm{ii}} > 0, \mathrm{i} = 1, 2, \cdots. \tag{20}$$

where $\{\psi_{\mathrm{i}}\}_{\mathrm{i=1}}^{\infty}$ denotes the function system in $W_2^2[0, T]$ obtained by

$$\begin{aligned} \psi_{\mathrm{i}}(x) &= A^* \kappa_{\mathrm{i}}(x) = \langle A^* \kappa_{\mathrm{i}}(\eta), S_{\mathrm{x}}(\eta)\rangle_{W_2^2} = \langle \kappa_{\mathrm{i}}(\eta), AS_{\mathrm{x}}(\eta)\rangle_{W_2^1} \\ &= \left\langle R_{\eta_{\mathrm{i}}}(\eta), AS_{\mathrm{x}}(\eta)\right\rangle_{W_2^1} = A_\eta S_{\mathrm{x}}(\eta)|_{\eta=\mathrm{x_i}}. \end{aligned} \tag{21}$$

And the coefficients $\varpi_{\mathrm{i}k}$ can be found by

$$\varpi_{\mathrm{ij}} = \begin{cases} \dfrac{1}{\|\psi_1\|}, & \text{for} \quad \mathrm{i} = \mathrm{j} = 1, \\ \dfrac{1}{e_{\mathrm{i}}}, & \text{for} \quad \mathrm{i} = \mathrm{j} \ne 1, \\ -\dfrac{1}{e_{\mathrm{i}}} \displaystyle\sum_{k=\mathrm{j}}^{\mathrm{i}-1} C_{\mathrm{i}k}\varpi_{k\mathrm{j}}, & \text{for} \quad \mathrm{i} > \mathrm{j}, \end{cases} \tag{22}$$

where $e_{\mathrm{i}} = (\|\psi_{\mathrm{i}}\|^2 - \sum_{k=1}^{\mathrm{i}-1} C_{\mathrm{i}k}^2)^{1/2}$, $C_{\mathrm{i}k} = \langle \psi_{\mathrm{i}}, \bar{\psi}_k\rangle_{W_2^2}$.

Theorem 9. *Suppose* $\{x_{\mathrm{i}}\}_{\mathrm{i=1}}^{\infty}$ *is dense in* $[0, T]$, *then* $\{\psi_{\mathrm{i}}\}_{\mathrm{i=1}}^{\infty}$ *is the complete system of* $W_2^2[0, T]$.

Proof. We know that $\psi_{\mathrm{i}}(\mathrm{x}) \in W_2^2[0, T]$. So, for each fixed $u(x) \in W_2^2[0, T]$, it follows

$$\langle u(x), \psi_{\mathrm{i}}(x)\rangle_{W_2^2} = 0, \ \mathrm{i} = 1, 2, \cdots. \tag{23}$$

Since

$$\begin{aligned} \langle u(x), \psi_{\mathrm{i}}(x)\rangle_{W_2^2} &= \langle u(x), A^* \kappa_{\mathrm{i}}(x)\rangle_{W_2^2} \\ &= \langle Au(x), \kappa_{\mathrm{i}}(x)\rangle_{W_2^1} \\ &= Au(x_{\mathrm{i}}) = 0, \end{aligned} \tag{24}$$

and $\{x_{\mathrm{i}}\}_{\mathrm{i=1}}^{\infty}$ is dense on the interval $[0, T]$, we have

$$Au(x) = 0. \tag{25}$$

Then,

$$A^{-1}(Au(x)) = A^{-1}(0), \tag{26}$$

that gives

$$u(x) = 0. \tag{27}$$

□

Lemma 10. *Assume $u \in W_2^2[0, T]$, then*

$$\left\| u^{(\mathfrak{i})}(x) \right\|_C \leq \mathfrak{C} \|u(x)\|_{W_2^2}, \quad \mathfrak{i} = 0, 1, \tag{28}$$

where $\mathfrak{C} \geq 0$ and $\|u(x)\|_C = \max_{x \in [0,T]} |u(x)|$.

Proof. $\forall x \in [0, T]$ we have

$$u^{(\mathfrak{i})}(x) = \left\langle u(\cdot), \partial_x^{(\mathfrak{i})} S_x(\cdot) \right\rangle_{W_2^2}, \quad \mathfrak{i} = 0, 1. \tag{29}$$

Using the expression of $\partial_x^{(\mathfrak{i})} S_x(\cdot)$, we can reach

$$\left\| \partial_x^{(\mathfrak{i})} S_x \right\|_{W_2^2} \leq \mathfrak{C}_{\mathfrak{i}}, \quad \mathfrak{i} = 0, 1. \tag{30}$$

Consequently,

$$\begin{aligned} \left| u^{(\mathfrak{i})}(x) \right| &= \left| \left\langle u(\cdot), \partial_x^{(\mathfrak{i})} S_x(\cdot) \right\rangle_{W_2^2} \right| \\ &\leq \left\| \partial_x^{(\mathfrak{i})} S_x \right\|_{W_2^2} \|u\|_{W_2^2} \\ &\leq \mathfrak{C}_{\mathfrak{i}} \|u\|_{W_2^2}, \mathfrak{i} = 0, 1. \end{aligned} \tag{31}$$

where $\mathfrak{C} = \max_{\mathfrak{i}=0,1} \{\mathfrak{C}_{\mathfrak{i}}\}$. Then Lemma 10 follows from (31). □

Theorem 11. *Assume $\{x_{\mathfrak{i}}\}_{\mathfrak{i}=1}^{\infty}$ is dense in $[0, T]$ and problem (18) has a solution that should be unique on $W_2^2[0, T]$. Therefore, the solution of (18) is*

$$u(x) = \sum_{\mathfrak{i}=1}^{\infty} \sum_{k=1}^{\mathfrak{i}} \varpi_{\mathfrak{i}k} \bar{F}(x_k, u(x_k)) \bar{\psi}_{\mathfrak{i}}(x). \tag{32}$$

While the solution of (14) is

$$f(x) = \sum_{\mathfrak{i}=1}^{\infty} \sum_{k=1}^{\mathfrak{i}} \varpi_{\mathfrak{i}k} \bar{F}(x_k, u(x_k)) \bar{\psi}_{\mathfrak{i}}(x) + \lambda. \tag{33}$$

Proof. Firstly, the fact that $\{\bar{\psi}_{\mathfrak{i}}(x)\}_{\mathfrak{i}=1}^{\infty}$ is a complete orthonormal basis in $W_2^2[0, T]$ allows us to write

$$\begin{aligned} u(x) &= \sum_{\mathfrak{i}=1}^{\infty} \langle u(x), \bar{\psi}_{\mathfrak{i}}(x) \rangle_{W_2^2} \bar{\psi}_{\mathfrak{i}}(x) \\ &= \sum_{\mathfrak{i}=1}^{\infty} \left\langle u(x), \sum_{k=1}^{\mathfrak{i}} \varpi_{\mathfrak{i}k} \psi_k(x) \right\rangle_{W_2^2} \bar{\psi}_{\mathfrak{i}}(x) \\ &= \sum_{\mathfrak{i}=1}^{\infty} \sum_{k=1}^{\mathfrak{i}} \varpi_{\mathfrak{i}k} \langle u(x), \psi_k(x) \rangle_{W_2^2} \bar{\psi}_{\mathfrak{i}}(x) \\ &= \sum_{\mathfrak{i}=1}^{\infty} \sum_{k=1}^{\mathfrak{i}} \varpi_{\mathfrak{i}k} \langle u(x), A^* \kappa_k(x) \rangle_{W_2^2} \bar{\psi}_{\mathfrak{i}}(x) \\ &= \sum_{\mathfrak{i}=1}^{\infty} \sum_{k=1}^{\mathfrak{i}} \varpi_{\mathfrak{i}k} \langle Au(x), \kappa_k(x) \rangle_{W_2^1} \bar{\psi}_{\mathfrak{i}}(x) \\ &= \sum_{\mathfrak{i}=1}^{\infty} \sum_{k=1}^{\mathfrak{i}} \varpi_{\mathfrak{i}k} \langle Au(x), R_x(x_k) \rangle_{W_2^1} \bar{\psi}_{\mathfrak{i}}(x) \\ &= \sum_{\mathfrak{i}=1}^{\infty} \sum_{k=1}^{\mathfrak{i}} \varpi_{\mathfrak{i}k} \bar{\mathrm{F}}(x_k, u(x_k)) \bar{\psi}_{\mathfrak{i}}(x), \end{aligned} \tag{34}$$

with $\bar{\mathrm{F}}(x_k, u(x_k)) = Au(\mathrm{x}_k)$.

Secondly, by replacing $g(\varsigma)$ by its formula (32) in the transformation (15), we get

$$u(x) = \sum_{\mathfrak{i}=1}^{\infty} \sum_{k=1}^{\mathfrak{i}} \varpi_{\mathfrak{i}k} \bar{\mathrm{F}}(x_k, u(x_k)) \bar{\psi}_{\mathfrak{i}}(x) + \lambda. \tag{35}$$

We now write the RKHSM's solution $u_n(x)$ as

$$u_n(x) = \sum_{\mathfrak{i}=1}^{n} \sum_{k=1}^{\mathfrak{i}} \varpi_{\mathfrak{i}k} \bar{\mathrm{F}}(x_k, u(x_k)) \bar{\psi}_{\mathfrak{i}}(x). \tag{36}$$

The space $W_2^2[0, T]$ is a Hilbert space, hence

$$\sum_{\mathfrak{i}=1}^{\infty} \sum_{k=1}^{\mathfrak{i}} \varpi_{\mathfrak{i}k} \bar{\mathrm{F}}(x_k, u(x_k)) \bar{\psi}_{\mathfrak{i}}(x) < \infty, \tag{37}$$

which means that $u_n(x)$ converges to $u(x)$ in the norm. □

Theorem 12.

(1) $u_n(x)$ converges uniformly to $u(x)$

(2) $u_n'(x)$ converges uniformly to $u'(x)$

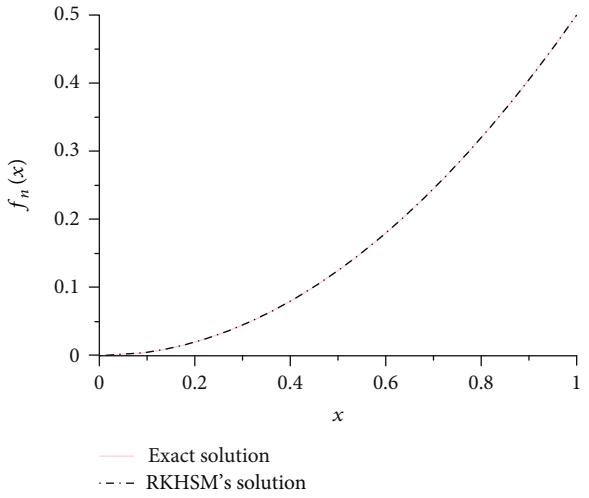

Figure 1: Exact and RKHSM's solutions for Example 1 with $g(x) = x$.

Proof. For the first result, we need to estimate the term on the left below:

$$\begin{aligned} &\forall x \in [0, T], \\ &|u_n(x) - u(x)| = \left|\langle u_n(\cdot) - u(\cdot), S_x(\cdot)\rangle_{W_2^2}\right| \\ &\qquad \le \|S_x\|_{W_2^2}\|u_n - u\|_{W_2^2} \\ &\qquad \le \mathscr{C}_0\|u_n - u\|_{W_2^2}, \end{aligned} \tag{38}$$

where $\mathscr{C}_0$ is a constant.

Following the same way, we get

$$\left|u_n'(x) - u'(x)\right| \le \|\partial_x S_x\|_{W_2^2}\left\|u_n' - u'\right\|_{W_2^2}, \tag{39}$$

due to the uniform boundedness of $\partial_x S_x(\cdot)$, we have

$$\|\partial_x S_x\|_{W_2^2} \le \mathscr{C}_1, \tag{40}$$

where $\mathscr{C}_1$ is a positive constant.

Therefore

$$\left|u_n'(x) - u'(x)\right| \le \mathscr{C}_1\left\|u_n' - u'\right\|_{W_2^2}. \tag{41}$$

□

4. A Numerical Experiment

This section is the numerical part that assures the efficiency of the proposed method by testing three examples. The rate of convergence of the presented method is as follows [18]:

$$(O_c)_n = \frac{-\ln\left(E_n/E_{n/2}\right)}{\ln(2)}, \tag{42}$$

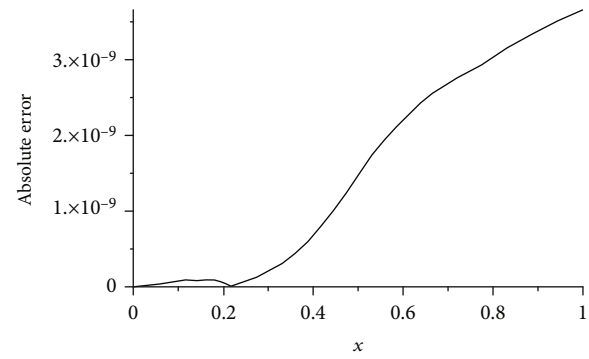

Figure 2: Absolute error of the RKHSM for Example 1 with $g(x) = x$.

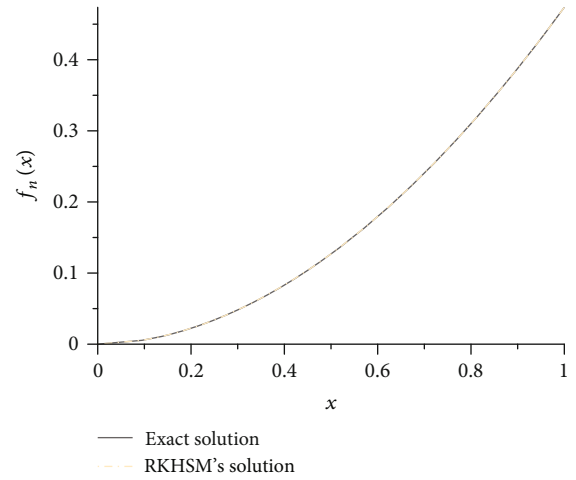

Figure 3: Exact and RKHSM's solutions for Example 1 with $g(x) = x^{0.9}$.

where

$$E_n = \max_{x\in[0,1]}|f(x) - f_n(x)|. \tag{43}$$

Now, how to apply the RKHSM can be summarized in the following procedure:

Step 1. Fix n.

Step 2. Set $\psi_{\mathfrak{i}}(x_{\mathfrak{i}}) = A_\eta S_x(\eta)\big|_{\eta=x_{\mathfrak{i}}}$.

Step 3. Calculate the orthogonalization coefficients $\varpi_{\mathfrak{i}\mathfrak{j}}$ using (22).

Step 4. Set $\bar{\psi}_{\mathfrak{i}}(x_{\mathfrak{i}}) = \sum_{k=1}^{\mathfrak{i}}\varpi_{\mathfrak{i}k}\psi_k(x_{\mathfrak{i}})$, $\varpi_{\mathfrak{i}\mathfrak{i}} > 0$, $\mathfrak{i} = 1, 2, \cdots, n$.

Step 5. Choose an initial guess $u_0(x_1)$.

Step 6. Set $\mathfrak{i} = 1$.

Step 7. Set $\Lambda_{\mathfrak{i}} = \sum_{k=1}^{\mathfrak{i}}\varpi_{\mathfrak{i}k}\bar{\mathrm{F}}(x_k, u(x_k))$.

Step 8. $u_{\mathfrak{i}}(x_{\mathfrak{i}}) = \sum_{\ell=1}^{\mathfrak{i}}\Lambda_\ell\bar{\psi}_\ell(x_\ell)$.

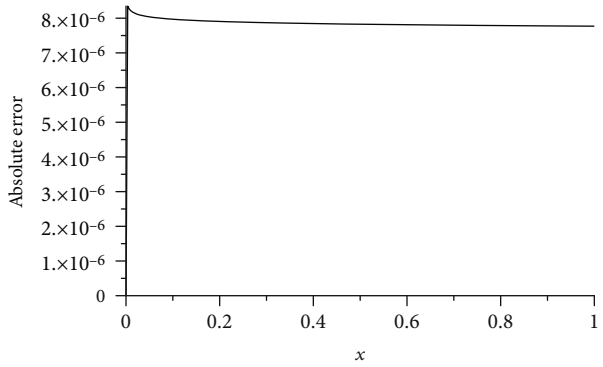

Figure 4: Absolute error of the RKHSM for Example 1 with $g(x) = x^{0.9}$.

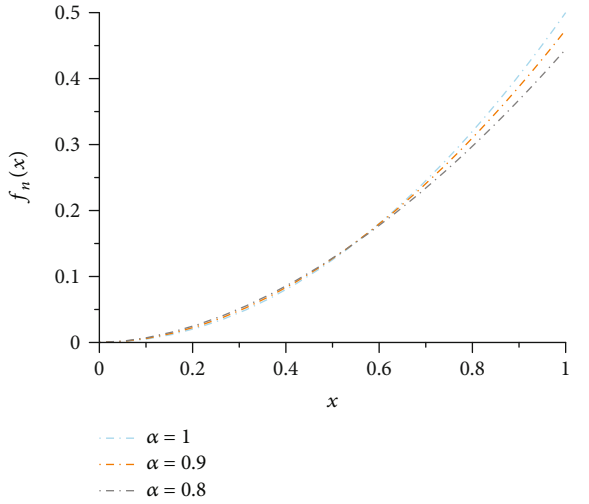

Figure 5: RKHSM's solutions for Example 1 with $g(x) = x^{\alpha}$: $\alpha = 1$, $\alpha = 0.9$, and $\alpha = 0.8$.

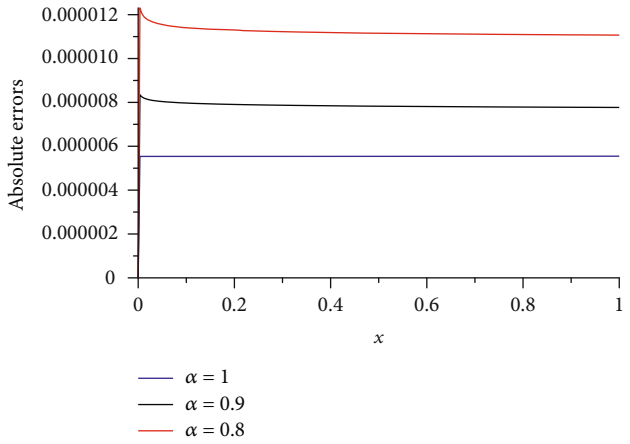

Figure 6: Absolute errors of the RKHSM for Example 1 with $g(x) = x^{\alpha}$ and $\alpha \in \{1; 0.9; 0.8\}$.

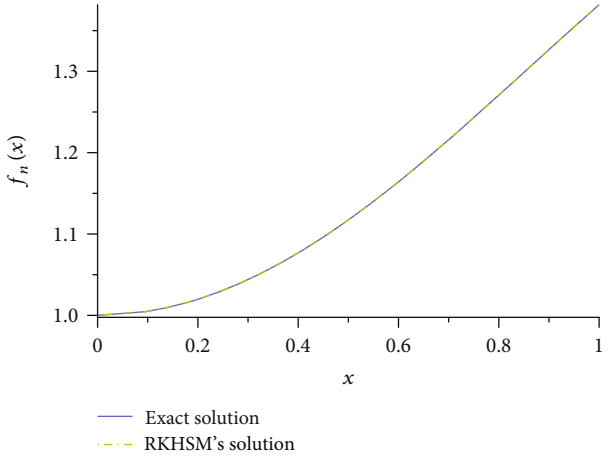

Figure 7: Exact and RKHSM's solutions for Example 1 with $g(x) = \sin(x)$.

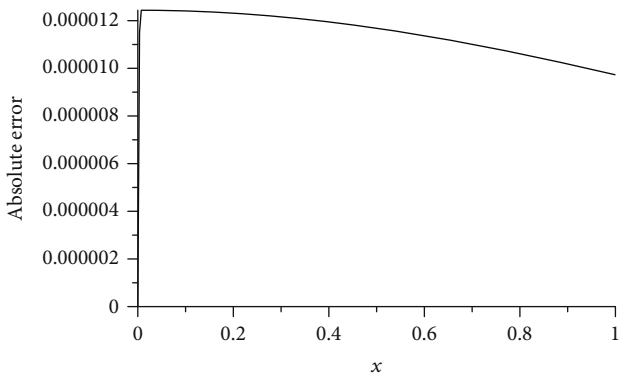

Figure 8: Absolute error of the RKHSM for Example 1 with $g(x) = \sin(x)$.

Table 1: Rate of convergence for Example 1 with $g(x) = x$.

n	Maximum absolute error	$(O_c)_n$
2	0.0833	——
4	0.0250	1.74
8	0.0069	1.85
16	0.0018	1.92
32	0.0005	1.96
64	0.0001	1.98
128	0.0000	1.99

Step 9. If $\mathbf{i} < n$, set $\mathbf{i} = \mathbf{i} + 1$. Go to Step 7. Else stop.

where $x_{\mathbf{i}} = \mathbf{i}/n$, $\mathbf{i} = 1, 2, \cdots, n$ and n is the number of collocation points.

Example 1. Taking the following linear ODE with global derivative:

$$\begin{cases} D_g f(x) = x, & x \in [0, 1], \\ f(0) = 0. \end{cases} \tag{44}$$

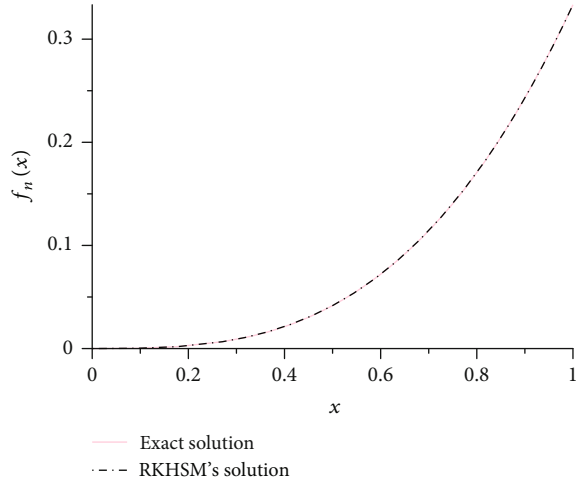

Figure 9: Exact and RKHSM's solutions for Example 2 with $g(x) = x$.

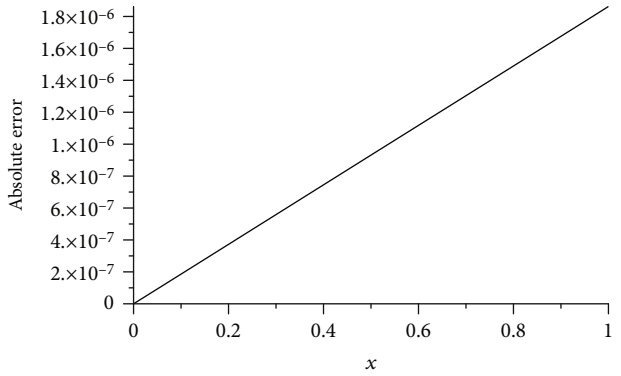

Figure 10: Absolute error of the RKHSM for Example 2 with $g(x) = x$.

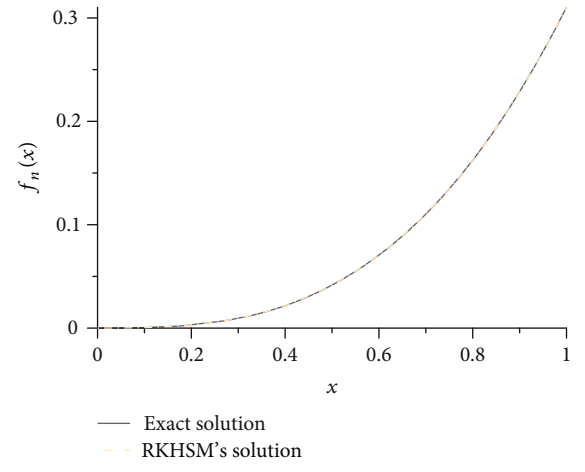

Figure 11: Exact and RKHSM's solutions for Example 2 with $g(x) = x^{0.9}$.

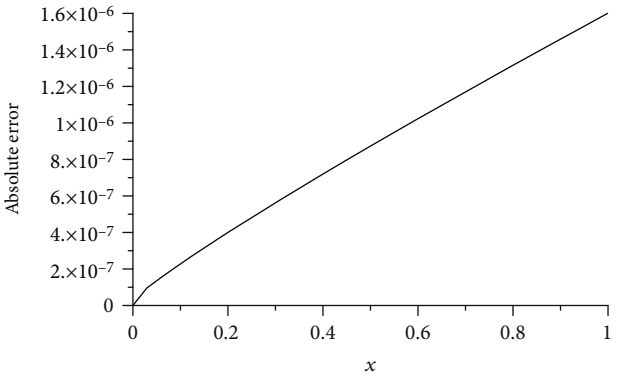

Figure 12: Absolute error of the RKHSM for Example 2 with $g(x) = x^{0.9}$.

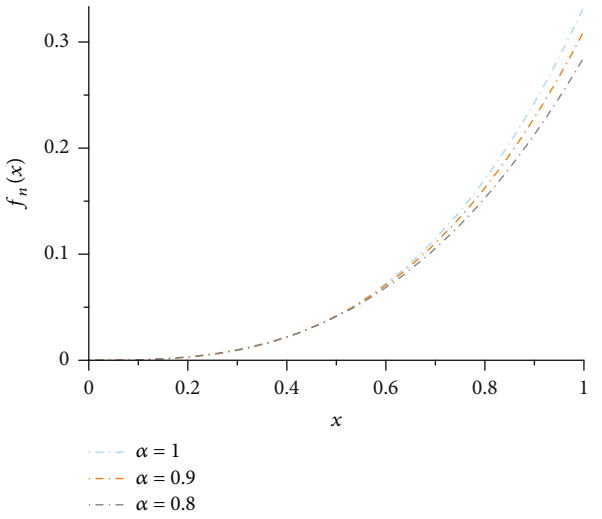

Figure 13: RKHSM's solutions for Example 2 with $g(x) = x^{\alpha}$: $\alpha = 1$, $\alpha = 0.9$, and $\alpha = 0.8$.

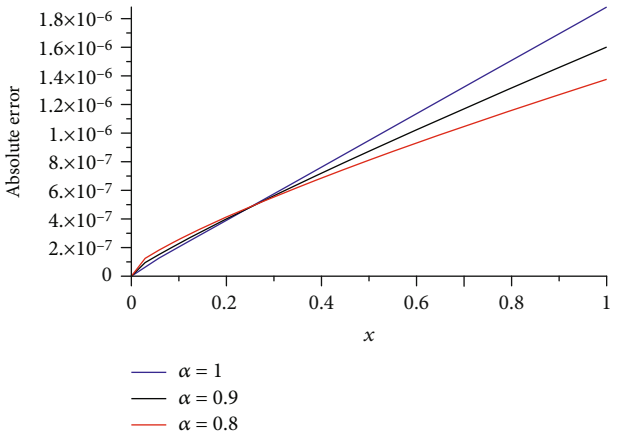

Figure 14: Absolute errors of the RKHSM for Example 2 with $g(x) = x^{\alpha}$ and $\alpha \in \{1\,; 0.9\,; 0.8\}$.

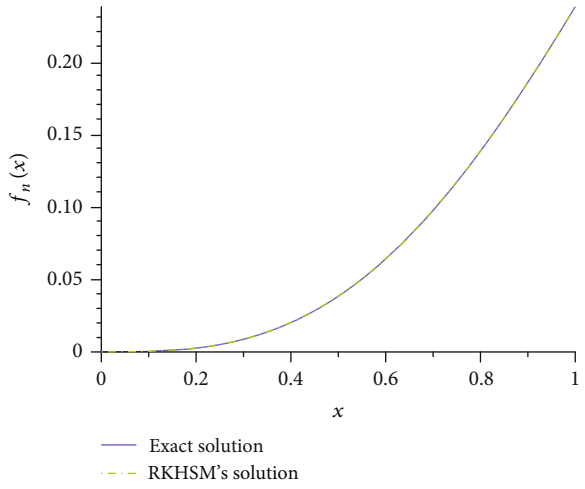

Figure 15: Exact and RKHSM's solutions for Example 2 with $g(x) = \sin(x)$.

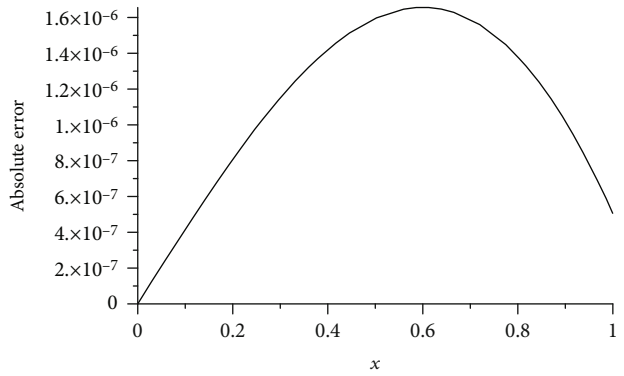

Figure 16: Absolute error of the RKHSM for Example 2 with $g(x) = \sin(x)$.

As the initial condition is homogeneous. We can then directly define a bounded linear operator A as

$$\begin{aligned} A : W_2^2[0,1] &\longrightarrow W_2^1[0,1] \\ f(x) &\longrightarrow Af(x) = D_g f(x). \end{aligned} \tag{45}$$

Taking $n = 100$ collocation points in which $x_i = i/n$, $i = 1, 2 \cdots, n$. The approximate solution for Example 1 is found using the RKHSM for different cases of the function $g(x)$ in the global derivative when $g(x)$ equals x,x^α, and $\sin(x)$. For each case, the results are compared with the exact solution. Figure 1 shows the exact solution and the RKHSM's solution with $g(x) = x$. The absolute error of this case is plotted in Figure 2. In Figure 3, we compared the exact solution with the RKHSM's solution when $g(x) = x^\alpha$ with $\alpha = 0.9$, and its absolute error is given in Figure 4, whereas in Figures 5 and 6, we depicted the obtained results for $\alpha = 1,0.9$, and 0.8 together. Figures 7 and 8 are where the results of the last case of $g(x)$ are given. We can see from these figures that the graphs' behavior is very similar. To highlight more comparisons between the RKHSM and the exact solution, we gave the rate of convergence for $g(x) = x$ in Table 1, and we drew

Table 2: Rate of convergence for Example 2 with $g(x) = x$.

n	Maximum absolute error	$(O_c)_n$
2	0.0833	——
4	0.0167	2.32
8	0.0035	2.26
16	0.0008	2.18
32	0.0002	2.11
64	0.0000	2.06

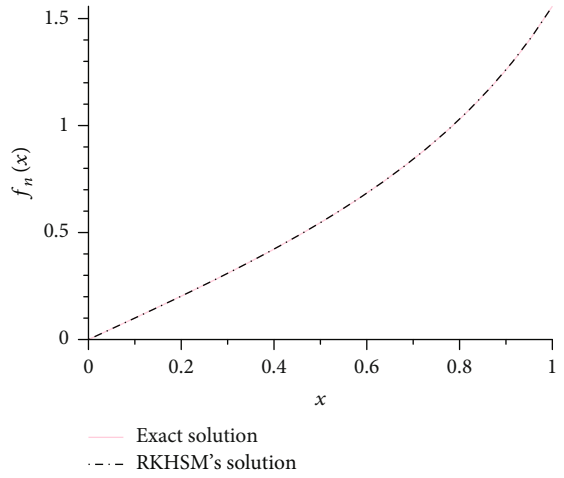

Figure 17: Exact and RKHSM's solutions for Example 3 with $g(x) = x$.

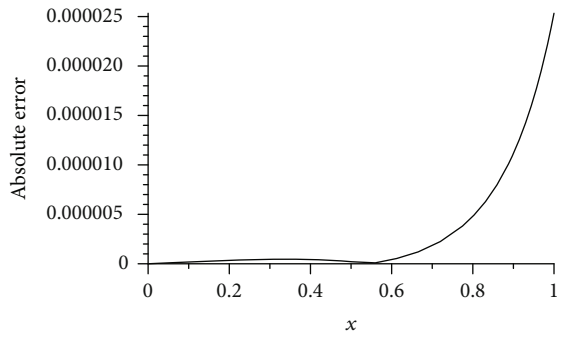

Figure 18: Absolute error of the RKHSM for Example 3 with $g(x) = x$.

the absolute error for each case through the figures presented. What we can observe here is that the RKHSM's solution is very close to the exact one. And this confirms that the proposed method is effective.

Example 2. Taking the following linear ODE with global derivative:

$$\begin{cases} D_g f(x) = x^2, & x \in [0,1], \\ f(0) = 0. \end{cases} \tag{46}$$

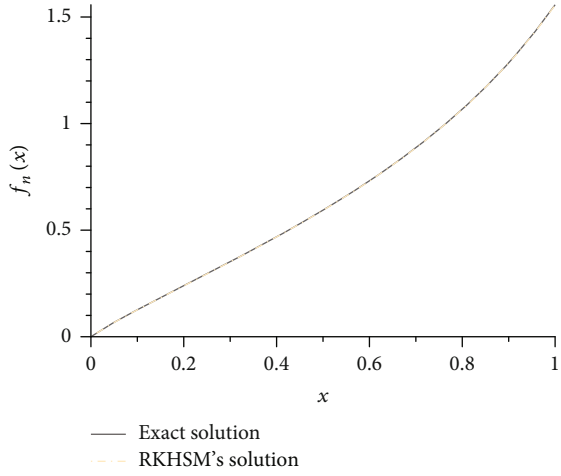

Figure 19: Exact and RKHSM's solutions for Example 3 with $g(x) = x^{0.9}$.

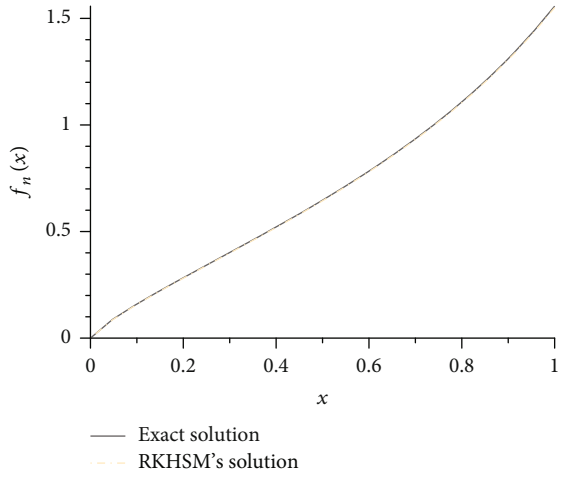

Figure 20: Exact and RKHSM's solutions for Example 3 with $g(x) = x^{0.8}$.

As the initial condition is homogeneous. We can then directly define a bounded linear operator A as

$$\begin{aligned} \mathrm{A} : W_2^2[0,1] &\longrightarrow W_2^1[0,1] \\ f(x) &\longrightarrow Af(x) = D_g f(x). \end{aligned} \tag{47}$$

Taking $n = 100$ collocation points in which $x = \mathfrak{i}/n$, $\mathfrak{i} = 1, 2 \cdots, n$. The approximate solution for Example 2 is found using the RKHSM for different cases of the function $g(x)$ in the global derivative when $g(x)$ equals x,x^α, and sin (x). For each case, the results are compared with the exact solution of each case. Figure 9 shows the exact solution and the RKHSM's solution with $g(x) = x$. The absolute error of this case is plotted in Figure 10. In Figure 11, we compared the exact solution with the RKHSM's solution when $g(x) = x^\alpha$ with $\alpha = 0.9$, and its absolute error is given in Figure 12, whereas in Figures 13 and 14, we depicted the obtained results for $\alpha = 1$,0.9, and 0.8 together. Figures 15 and 16 are where the results of the last case of $g(x)$ are given. We can see from these figures that the graphs' behavior is very similar. To highlight more comparisons between the RKHSM and the exact solution, we gave the rate of convergence for $g(x) = x$ in Table 2, and we drew the absolute error for each case through the figures presented. What we can observe here

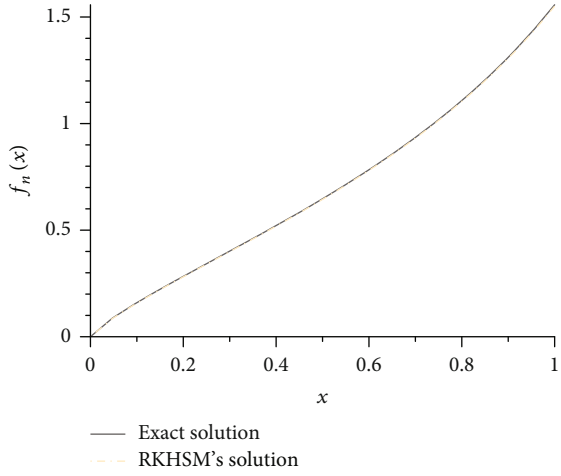

Figure 21: Exact and RKHSM's solutions for Example 3 with $g(x) = x^{0.6}$.

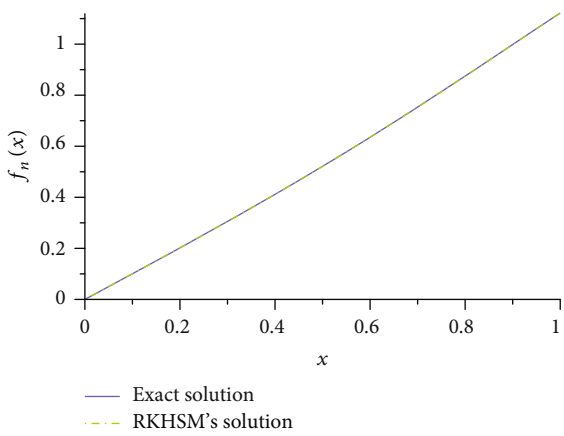

Figure 22: Exact and RKHSM's solutions for Example 3 with $g(x) = \sin(x)$.

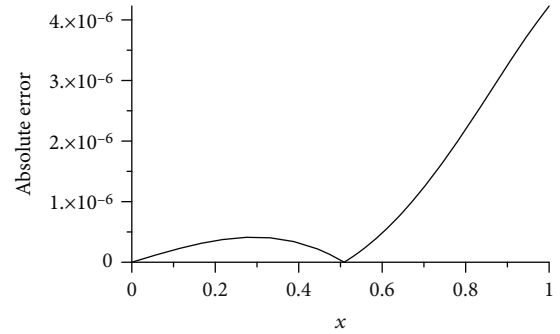

Figure 23: Absolute error of the RKHSM for Example 3 with $g(x) = \sin(x)$.

Table 3: Rate of convergence for Example 3 with $g(x) = x$.

n	Maximum absolute error	$(O_c)_n$
2	0.1027	——
4	0.0658	0.64
8	0.0260	1.34
16	0.0078	1.73
32	0.0021	1.89
64	0.0005	1.95

is that the RKHSM's solution is very close to the exact one. And this confirms that the proposed method is effective.

Example 3. Taking the following linear ODE with global derivative:

$$\begin{cases} D_g f(x) = f(x)^2 + 1, & x \in [0, 1], \\ f(0) = 0. \end{cases} \tag{48}$$

As the initial condition is homogeneous. We can then directly define a bounded linear operator A as

$$\begin{aligned} A : W_2^2[0, 1] &\longrightarrow W_2^1[0, 1] \\ f(x) &\longrightarrow Af(x) = D_g f(x). \end{aligned} \tag{49}$$

Taking$n = 100$ collocation points in which $x = \mathfrak{i}/n$, $\mathfrak{i} = 1, 2 \cdots, n$. The approximate solution for Example 3 is found using the RKHSM for different cases of the function $g(x)$ in the global derivative when $g(x)$ equals x,x^α, and sin (x). For each case, the results are compared with the exact solution of each case. Figure 17 shows the exact solution and the RKHSM's solution with $g(x) = x$. The absolute error of this case is plotted in Figure 18. In Figures 19–21, we compared the exact solution with the RKHSM's solution when $g(x) = x^\alpha$ with $\alpha \in \{0.9,0.8,0.6\}$. Figures 22 and 23 are where the results of the last case of $g(x)$ are given. We can see from these figures that the graphs' behavior is very similar. To highlight more comparisons between the RKHSM and the exact solution, we gave the rate of convergence for $g(x) = x$ in Table 3, and we drew the absolute error for each case through the figures presented. What we can observe here is that the RKHSM's solution is very close to the exact one. And this confirms that the proposed method is effective.

5. Conclusion

In this paper, an efficient method, named the reproducing kernel Hilbert space method, is applied successfully for solving nonlinear ODEs described by using the global derivative. The accuracy and applicability of the RKHSM are validated by computing the numerical solutions at many grid points. The results show that the RKHSM is a powerful method to deal with many other nonlinear problems that arise in a large variety of physical problems with different types of derivatives.

Data Availability

All of the necessary data and the implementation details have been included in the manuscript.

Conflicts of Interest

The authors declare that they have no conflicts of interest.

References

[1] S. Zaremba, "Sur le calcul numérique des fonctions demandées dans le problème de Dirichlet et le problème hydrodynamique," *Bulletin International de l'Académie des Sciences de Cracovie*, vol. 68, pp. 125–195, 1908.

[2] O. Abu Arqub, J. Singh, B. Maayah, and M. Alhodaly, "Reproducing kernel approach for numerical solutions of fuzzy fractional initial value problems under the Mittag–Leffler kernel differential operator," *Mathematical Methods in the Applied Sciences*, 2021.

[3] T. Allahviranloo and H. Sahihi, "Reproducing kernel method to solve fractional delay differential equations," *Applied Mathematics and Computation*, vol. 400, article 126095, 2021.

[4] E. Babolian, S. Javadi, and E. Moradi, "RKM for solving Bratu-type differential equations of fractional order," *Mathematical Methods in the Applied Sciences*, vol. 39, no. 6, pp. 1548–1557, 2016.

[5] Y. Chellouf, B. Maayah, S. Momani et al., "Numerical solution of fractional differential equations with temporal two-point BVPs using reproducing kernal Hilbert space method," *AIMS Mathematics*, vol. 6, no. 4, pp. 3465–3485, 2021.

[6] M. Foroutan, A. Ebadian, and H. R. Fazli, "Generalized Jacobi reproducing kernel method in Hilbert spaces for solving the Black-Scholes option pricing problem arising in financial modelling," *Mathematical Modelling and Analysis*, vol. 23, no. 4, pp. 538–553, 2018.

[7] F. Geng and M. Cui, "New method based on the HPM and RKHSM for solving forced Duffing equations with integral boundary conditions," *Journal of Computational and Applied Mathematics*, vol. 233, no. 2, pp. 165–172, 2009.

[8] F. Geng and M. Cui, "A reproducing kernel method for solving nonlocal fractional boundary value problems," *Applied Mathematics Letters*, vol. 25, no. 5, pp. 818–823, 2012.

[9] N. Harrouche, S. Momani, S. Hasan, and M. Al-Smadi, "Computational algorithm for solving drug pharmacokinetic model under uncertainty with nonsingular kernel type Caputo-Fabrizio fractional derivative," *Alexandria Engineering Journal*, vol. 60, no. 5, pp. 4347–4362, 2021.

[10] F. Hemati, M. Ghasemi, and G. R. Khoshsiar, "Numerical solution of the multiterm time-fractional diffusion equation based on reproducing kernel theory," *Numerical Methods for Partial Differential Equations*, vol. 37, pp. 44–68, 2021.

[11] W. Jiang and T. Tian, "Numerical solution of nonlinear Volterra integro-differential equations of fractional order by the reproducing kernel method," *Applied Mathematical Modelling*, vol. 39, no. 16, pp. 4871–4876, 2015.

[12] S. Momani, N. Djeddi, M. Al-Smadi, and S. Al-Omari, "Numerical investigation for Caputo-Fabrizio fractional Riccati and Bernoulli equations using iterative reproducing kernel method," *Applied Numerical Mathematics*, vol. 170, pp. 418–434, 2021.

[13] M. G. Sakar, "Iterative reproducing kernel Hilbert spaces method for Riccati differential equations," *Journal of Computational and Applied Mathematics*, vol. 309, pp. 163–174, 2017.

[14] E. N. Yildirim, A. Akgül, and M. Inc, "Reproducing kernel method for the solutions of non-linear partial differential equations," *Arab Journal of Basic and Applied Sciences*, vol. 28, no. 1, pp. 80–86, 2021.

[15] A. Atangana, "Extension of rate of change concept: from local to nonlocal operators with applications," *Results in Physics*, vol. 19, article 103515, 2020.

[16] M. Cui and Y. Lin, "Nonlinear numerical analysis in the reproducing kernel space," Nova Science Publishers, Inc, New York, 2009.

[17] N. Attia, A. Akgül, D. Seba, and A. Nour, "An efficient numerical technique for a biological population model of fractional order," *Chaos, Solitons and Fractals*, vol. 141, article 110349, 2020.

[18] E. Babolian, S. Javadi, and E. Moradi, "Error analysis of reproducing kernel Hilbert space method for solving functional integral equations," *Journal of Computational and Applied Mathematics*, vol. 300, pp. 300–311, 2016.